Experimental Validation of the Seismic Performance of a Foldable Steel Unit House

Ryosuke MATSUDA
Candidate for the Degree of Master of Engineering
Supervisor: Dr. Taichiro Okazaki
Division of Architectural and Structural Design

Introduction

Unit houses are a modular prefabricated steel building system which can be constructed and disassembled in a short period of time, can be reused multiple times, and achieves low-price construction. In Japan, the use of unit houses is limited primarily to temporary, construction-site offices. However, if combined with appropriate exterior panels, unit houses can be used for ordinary houses or buildings. The rapid hospital construction in Wuhan City, China was a notable use of unit houses. Wang et al. [1] examined the cyclic-loading performance of a unit-house framing system assembled into two stories. Other than this exception, research on the structural performance of unit houses has focused on their beam-to-column connections and vertical joints between units. The contribution of non-structural components on the performance of unit houses is not well understood [2]. Therefore, shake-table tests were conducted on a unit house product manufactured by FUJI SASH CO., Ltd. in December 2019 and November 2020. The shake-table test program along with key findings are reported herein.

Overview of Unit House

Commercial unit-house products “SK 5700” and “SK 7500” produced by FUJI SASH CO., Ltd. [3], were examined. The products are 5.5 m × 2.2 m and 7.3 m × 2.2 m, respectively, in floor area and 2.7-m high. Each unit is completed with roof finish, floor finish, furring columns, and electronic wiring. As shown in Figure 1, the units consist of two short-side frames, which are identical between SK 5700 and SK 7500, a roof frame, and a floor frame. In the longer direction, SK 7500 is 32% longer than SK 5700. The unit is folded for transportability and unfolded on site. Unfolding is done by pulling the roof frame upward while rotating the short-side frame about a pivot. The units may be connected horizontally and vertically as needed. A unit-house building is completed by installing external wall panels along its perimeter. Various types of external wall panels are available to accommodate a wide range of architectural uses.

The columns are cold-formed hollow structural sections 100×100×4.5 (STKR400); the beams are cold formed from hot-dip galvanized steel sheets SGH400 of thickness 3.2 or 4.5 mm. Figure 2 shows representative beams and beam-to-column connections. The beams adopt an open, non-symmetrical section to support the external wall panels. Rigid beam-to-column connections are achieved by CJP welds in the short-side frames and by slip-critical bolted connections through 12-mm gusset plates in the long-side frame. For the latter, three and four M16-S10T high-strength, tension-controlled bolts are used, respectively, at the top and bottom

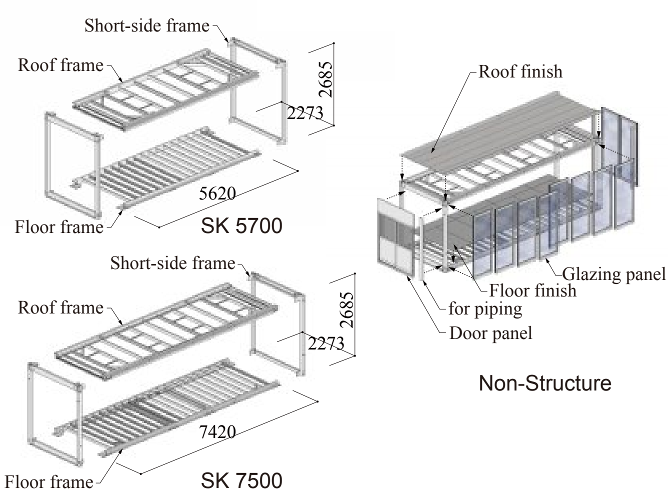

Figure 1. Structural frame and compositon of the unit house

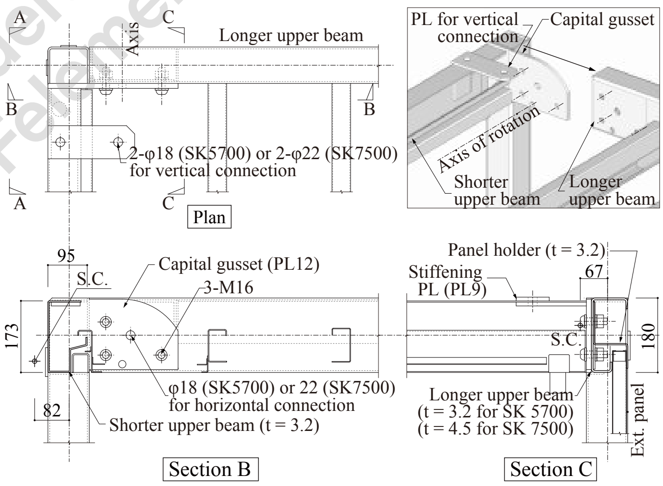

(a) Upper beam-to-column connection

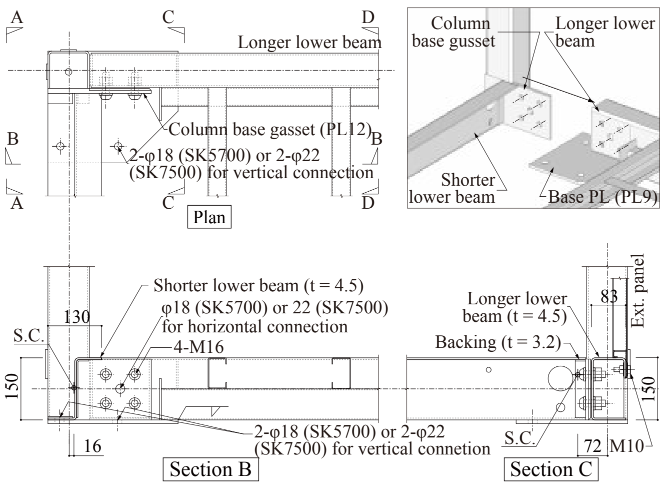

(b) Lower beam-to-column connection

Figure 2. Member arrangement and beam-to-column connections

connections. The faying surface is blast cleaned and coated with a thick-film inorganic zinc-rich paint.

Wall panels are fitted into an upper beam and fixed to a lower beam using two M10 bolts. Plastic packing is fitted between the panels and between the end panel and column to ensure airtightness and watertightness. The 10-mm gap between the end panel and column is exhausted when the story drift angle reaches 0.0042 rad. The contribution of wall panels and furring columns to lateral-load resistance is neglected in structural design.

Shake-Table Test Plan

Shake-table tests were conducted at the Large-Scale Earthquake Simulator of the National Research Institute for Earth Science and Disaster Resilience (NIED). Three specimens each comprising 4 units connected vertically and horizontally were constructed and fixed on the shake-table through a steel foundation system. Specimens 1 and 2 used SK 5700 units and Specimen 3 used SK 7500 units. Steel plates weighting 1,870 kg total were glued to the floor finish of each second-floor unit. The weight equaled 189 and 135%, respectively, for SK 5700 and SK 7500, of the live load to compute design earthquake loads for office use (800 N/m^2).

As shown in Figure 3, Specimens 1 and 3 were loaded in the long-frame direction while Specimen 2 was loaded in the short-frame direction. The fundamental vibration periods of Specimens 1, 2, and 3 were computed as 0.41, 0.35, and 0.48 s, in the respective loading directions. The same mix of wall panels were installed in both floors. For Specimen 1, the south and north walls had a window panel and four solid panels; the east wall had a window panel and two solid panels; the west wall had a window panel and a door panel. Specimen 2 used the same combination as Specimen 1. For Specimen 3, the south and east walls had eight and four glazing panels, respectively; the north wall had eight solid panels; the west wall had two solid panels and a door panel.

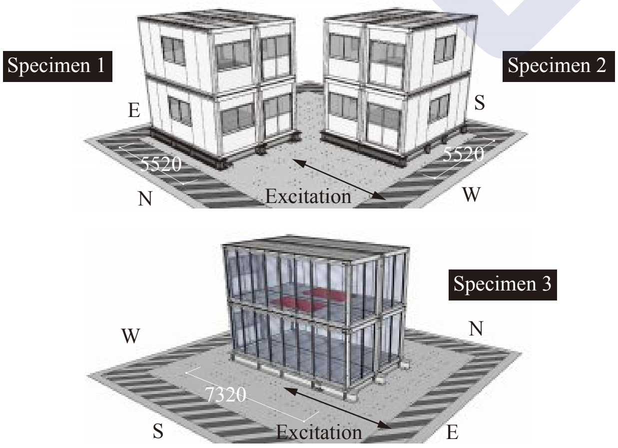

Figure 3. Specimens placed on shake table

The NS component of the JMA Kobe record from the 1995 Kobe earthquake was repeated nine times, amplified to 10, 25, 10, 50, 10, 100, 10, 100, and 10%. For the fundamental vibration periods of the specimens, the acceleration response spectrum of the 50% motion was equivalent to the design spectrum specified for Level 2 Design, which is generally intended for a return period of 500 years.

Shake-Table Test Results

No structural damage was observed up to the 50% excitation. Modest damage to the external wall panels was noted in Specimen 1 such as hole elongation of the surface steel sheets at the bottom bolts.

After the first 100% excitation, structural damage was observed at the first story of Specimens 1 and 2. In Specimen 1, bending deformation was observed in the column base plates, which was exacerbated by eccentricity between the anchor bolts and column. In Specimen 2, weld cracks were observed at the connections between the lower beam and column (Figure 4 (a)). No structural damage was observed in Specimen 3. Damage to the external wall panels was extensive in Specimens 1 and 2, but very minor in Specimen 3: In Specimen 1, the damage took form of pull-out failure of the surface steel sheets at the bottom bolts, and deformation near the upper corner due to contact with the column (Figure 4 (b)); In Specimen 2, the panel had partly come off near the upper corner and around window openings, more badly on the north side where the window was larger (Figure 4 (c)). After the second 100% excitation, the same damage developed further. During dismantling after the test, wide-spread occurrence of local buckling deformation was noticed in the upper beams of the short-side frame (Figure 4 (d)).

Figure 5 plots the relationships between shear force and drift ratio measured for the first story during the first 100% excitation. Story shear was computed based on the assumed mass and measured floor acceleration. Indicated in the figure are the computed elastic stiffness of the system, story shear H_{y1} and H_{y2} at the elastic limit determined by column yielding, based on nominal yield strength and yield strength reported in mill-test reports, respectively, drift ratio where the column was expected to contact the wall panels, and state points before and after excitation. During the first 100% excitation, Specimens 1 and 3 behaved similarly between the north and south frames, while Specimen 2 deformed more in the north frame, which had larger window openings, than the south frame, which had smaller window openings. All specimens exhibited large loading and unloading stiffness when the drift ratio exceeded 0.01 rad. Residual drift ratio did not exceed 0.005 rad. Specimen 3 exhibited, whenever the drift ratio changed signs from positive to negative or vice versa, stagnation or decrease in story shear followed by sharp increase.

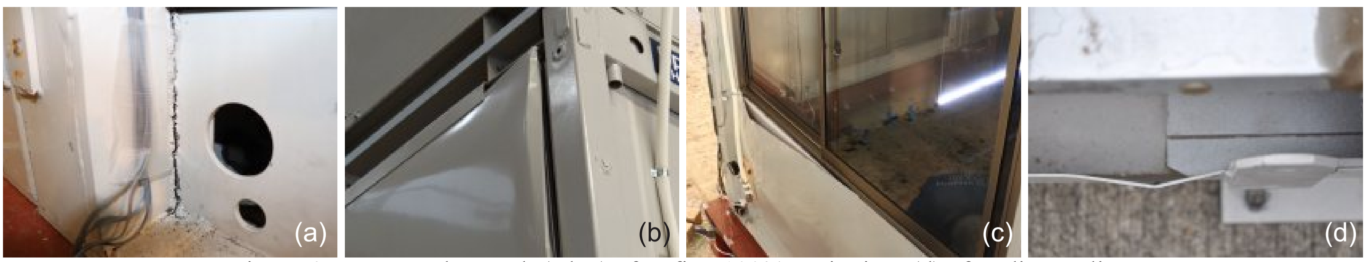

Figure 4. Damage observed: (a,b,c) after first 100% excitation; (d) after dismantling

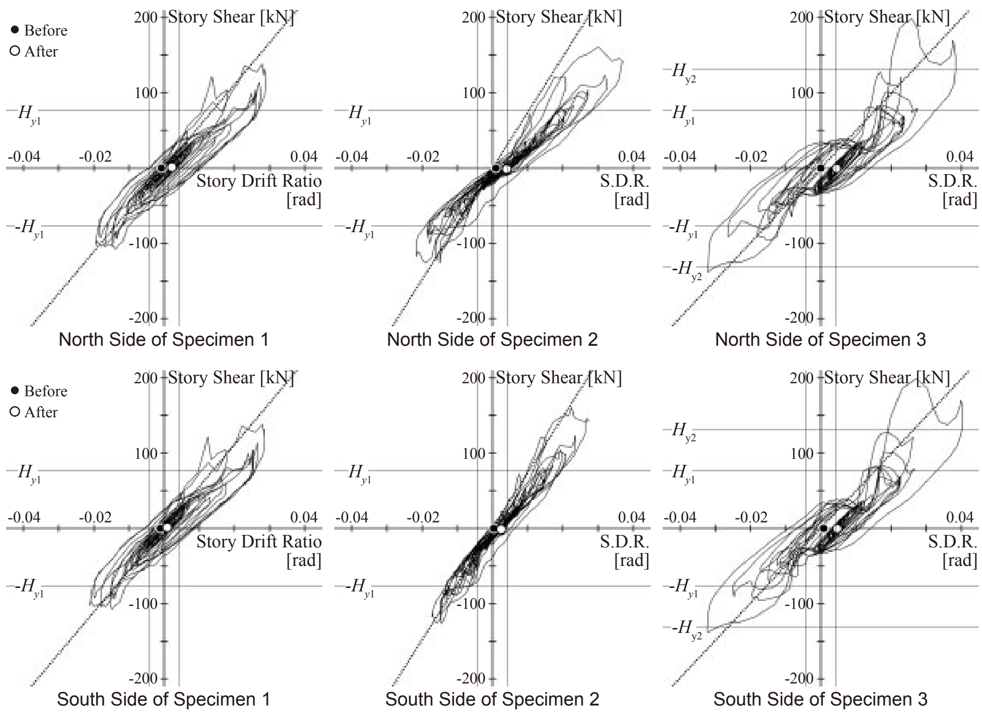

Figure 5. Story shear versus drift ratio of first floor during first 100% excitation

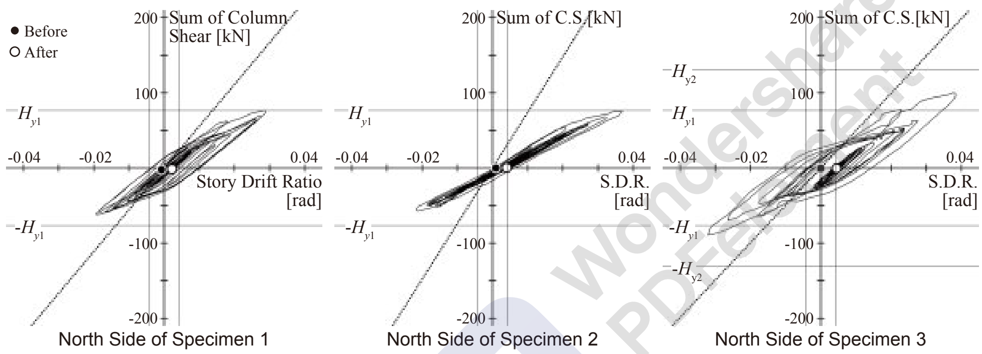

Figure 6. Sum of column shear versus drift ratio of first floor during first 100% excitation

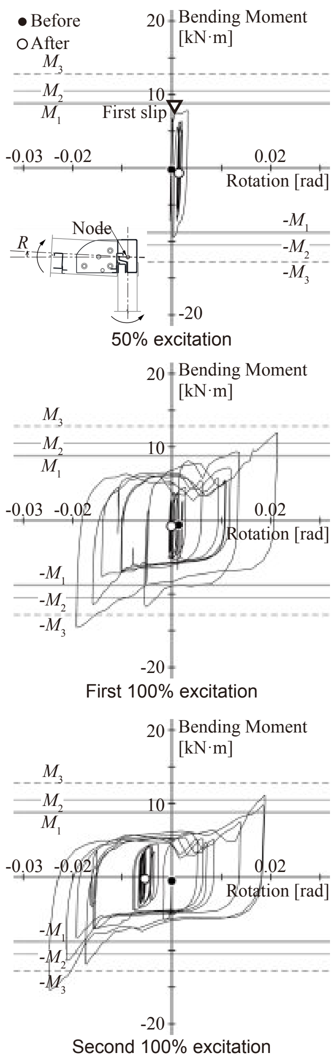

Figure 7. Bending moment versus slip rotation angle of slip-critical bolted connection

Figure 6 shows the relationship between sum of column shear and drift ratio measured for the first story during the first 100% excitation. Column shear was deduced from strain gauge measurement and equilibrium. Drift ratio was represented by the north frame. The elastic stiffness was 80%, 40%, and 90% of the computed stiffness for Specimens 1, 2, and 3, respectively. The reason why Specimen 2 exhibited much smaller stiffness than the computed value is believed to be due to local buckling in the upper beam. Specimens 1 and 3 exhibited apparent elastic-plastic behavior, which, as discussed later, was due to repeated slipping at the slip-critical bolted connections. Specimen 2 behaved more linearly. The difference in shear force between Figure 5 and Figure 6 are attributed primarily to the resistance of external wall panels. Panels contributed to lateral resistance to the same extent as structural frame when deformation exceeded 0.02 rad. Although not reported here, data suggests that the stagnation or decrease followed by sharp increase of shear force, observed in Figure 5, was associated with contact and separation of the wall panels from the columns and slip at vertical connections between the upper-story and lower-story modules.

Figure 7 shows the relationship between bending moment evaluated at the beam-to-column node and slip rotation angle of a slip-critical bolted connection measured during the 50% and 100% excitations. The sampled location was at the first-story upper beam in the south-west corner of Specimen 3. The nominal slip resistances M_1 and M_2, were computed according to the instantaneous center-of-rotation method [4], and conventional method. The slip resistance of a single bolt was calculated as the product of nominal bolt pretension and slip coefficient 0.45. The nominal column yield moment M_3, and the state points before and after excitation, and at first slip, are indicated in the figure. The first positive and negative slips occurred during the 50% excitation at 70 to 80% of M_1. Many more positive and negative slips occurred during the 100% excitation, resulting in gradual strength decrease. A steady state was reached after 5 total slips, when the slip resistance had reduced to half of the initial resistance.

Similar behavior was observed at all measured locations, two and eight, respectively, for Specimens 1 and 3. Based on integration over the respective hysteresis, for the first 100% excitation, the energy dissipated by the slip-critical connections was 82% and 88%, respectively, of the total dissipated energy for Specimen 1 and 3.

According to literature, slip-critical bolted connections with inorganic zinc-rich paint applied to the faying surface tends to exhibit smaller than nominal slip resistance because the decrease in bolt pretension tends to be larger compared to cases where such paint is not used [5]. It is also reported [6] that the slip resistance of such connections tends to decrease with each slip until a steady value is reached.

Figure 8 shows transition of maximum story shear and story drift of first story in each specimen. For the 10% to the first 100% excitation, story shear was 20% larger in Specimen 3 than in Specimen 1. This difference corresponded to the different in mass of the second floor. For the second 100% excitation, the story shear were equal between Specimens 1 and 3, presumably because they reached the strength, equal between the specimens, determined by the slip resistance of slip-critical bolted connections. The story drifts were similar in all specimens until the 50% excitation. During the second 100% excitation, all 3 specimens deformed to 0.04 rad.

Beam-to-Column Connections Tests

To further understand the performance limits of the system, isolated beam-to-column connection specimens were tested. Four types of L-shape specimens were constructed, each corresponding to different locations in product SK 5700. Figure 9 illustrates a specimen which represented the upper connection in the long-side frame. Specimens were simply supported, and were subjected to either monotonic tension, monotonic compression, or cyclic tension and compression. Cyclic loading was controlled in reference to load P_d that equaled the design load effect determined by either earthquake or wind load.

The specimens exhibited excellent performance in the range of cyclic deformation observed in the aforementioned shake-table tests, ±0.04 rad. All specimens remained elastic at $\pm 1.0P_d$ and sustained load nearly ten times P_d at 0.07 rad. The slip-critical bolted connections in the longer frame exhibited repeated slip, as in Figure 7, with gradual reduction in slip resistance at each slip. The welded upper connection in the shorter frame twisted under tension, and buckled at the unsupported edge of the section. It was confirmed by analysis that this section inherently develops large warping torsion due to its geometry and eccentricity between its shear center and line of load application. This behavior agreed with observation in the shake-table tests where all upper beams had

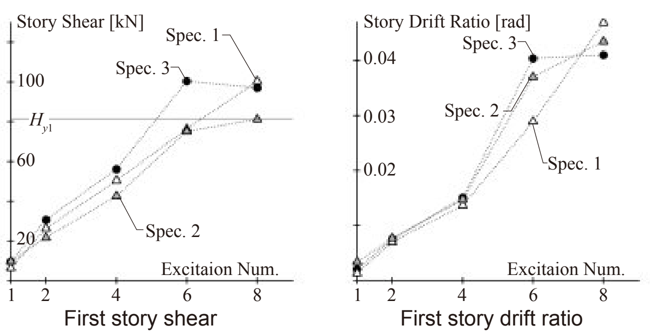

Figure 8. Specimens placed on shake table

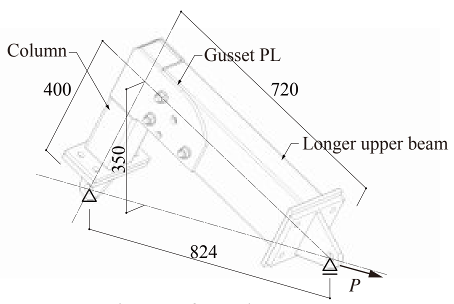

Figure 9. Specimens from longer upper connections

buckled at the same location (see Figure 4 (d)). Portal frame tests are under preparation to complement the findings.

Conclusions

Shake-table tests were conducted to examine the seismic performance of two unit-house products furbished with external wall panels. Three specimens were constructed, each comprising four units joined horizontally and vertically to form a two-story building. Different types of wall panels were installed along the perimeter. The specimens were subjected to the JMA Kobe-NS record nine times, with different amplification factors.

After the 50% excitation, which corresponds to Level-2 seismic design requirement, no structural damage and no residual drift was observed. The 100% excitation caused a maximum drift ratio of 0.04 rad, but resulted in residual drift less than 0.005 rad. After the 100% excitation, structural damage was observed in the specimen shaken in the short-side direction: Weld cracks and fracture in the lower beams and substantial local buckling deformation in the upper beams.

Deformation in the long-side frame concentrated in the slip-critical bolted connections. The slip resistance decreased after each slip, until reducing to half of the initial resistance. The energy dissipated by repeated slip at the slip-critical bolted connections accounted for more than 80% of the total energy dissipated by the structural system.

Non-structural external wall panels contributed 20% to 30% to the lateral stiffness of the structural system in the elastic response region, and nearly doubled the lateral resistance of the structural system for a moment when the drift ratio exceeded 0.02 rad.

Component tests suggested that the beam-to-column connections of the unit houses can exhibit excellent performance to double the cyclic deformation range in the shake-table tests.

Acknowledgements

The shake-table test was done in collaboration with Nagoya University, Kindai University, Tohoku University, FUJI SASH CO. Ltd., Iijima structural design office, INVISIBLE design, and NIED. The contribution of students from all participating universities are appreciated.

References

[1] Xiandun Wang et al. Seismic performance of ATLS modular house based on joint stiffness analysis. *Journal of Constructional Steel Research*. Vol. 183. 2021. *doi:*10.1016/j.tws.2021.107625

[2] En-Feng Deng et al. Seismic performance of mid-to-high rise modular steel construction -A critical review-. *Thin-Walled Structures*. Vol. 155. 2020. *doi:*10.1016/j.tws.2020.106924

[3] FUJI SASH Homepage. Unispace series. <http://www.fujisash.co.jp/hp/product/unit/unispace/sk/>. last accessed 2020/11/7. (in Japanese).

[4] AISC. Steel construction manual. 13th edition. 2010.

[5] Hwan-Seon Nah et al. Evaluating long term relaxation of high strength bolts considering coating on slip faying surface. *Steel and Composite Structures*. Vol. 16. No. 6. pp. 703-718. 2014.

[6] Yasuhiro Ishihara et al. Characteristic investigation and cyclic slip experiment of HSFG bolted joints which were damaged by earthquake. *Journal of Japan Society of Civil Engineers*. No. 745. I-65. pp. 53-64. 2003. (in Japanese).